

Part 1: Theory

S. P. Carter et al.

This discussion paper is/has been under review for the journal The Cryosphere (TC).  
Please refer to the corresponding final paper in TC if available.

# Active lakes in Antarctica survive on a sedimentary substrate – Part 1: Theory

S. P. Carter, H. A. Fricker, and M. R. Siegfried

Institute of Geophysics and Planetary Physics, Scripps Institution of Oceanography,  
University of California, San Diego, CA, USA

Received: 21 January 2015 – Accepted: 21 January 2015 – Published: 26 March 2015

Correspondence to: S. P. Carter (spcarter@ucsd.edu)

Published by Copernicus Publications on behalf of the European Geosciences Union.

Title Page

Abstract

Introduction

Conclusions

References

Tables

Figures



Back

Close

Full Screen / Esc

Printer-friendly Version

Interactive Discussion



## Abstract

Over the past decade satellite observations have revealed that active subglacial lake systems are widespread under the Antarctic ice sheet, including the ice streams, yet we have insufficient understanding of the lake-drainage process to incorporate it into ice sheet models. Process models for drainage of ice-dammed lakes based on conventional “R-channels” incised into the base of the ice through melting are unable to reproduce the timing and magnitude of drainage from Antarctic subglacial lakes estimated from satellite altimetry given the low hydraulic gradients along which such lakes drain. We developed a process model in which channels are mechanically eroded into deformable subglacial sediment (till) instead (“T-channel”). When applied to the known lakes of the Whillans/Mercer system, the model successfully reproduced the key characteristics of estimated lake volume changes for the period 2003–2009. If our model is realistic, it implies that most active lakes are shallow and only exist in the presence of saturated sediment, explaining why they are difficult to detect with classical radar methods. It also implies that the lake-drainage process is sensitive to the composition and strength of the underlying till, suggesting that models could be improved with a realistic treatment of sediment – interfacial water exchange.

## 1 Introduction

Since the initial observation of “large flat circular basins” on the ice surface of the ice by Russian pilots during International Geophysical year (Robinson, 1964) and the inference of those basins as lakes beneath the ice sheet, there have been over 300 subglacial lakes discovered throughout the continent using a variety of geophysical methods (Wright and Siegert, 2012). Until the mid 2000’s radio echo sounding (RES) was the primary technique for identifying subglacial lakes (Carter et al., 2007; Siegert et al., 2007), and this method confirmed that many of the anomalously flat features previously identified on the ice surface resulted from the long term storage of free water

Title Page

Abstract

Introduction

Conclusions

References

Tables

Figures



Back

Close

Full Screen / Esc

Printer-friendly Version

Interactive Discussion



at the ice sheet base, including Lake Vostok (Ridley et al., 1993), which measures over 12 500 km<sup>2</sup> in area (Kapitsa et al., 1996). With most of the lakes identified through RES and active seismic surveys located beneath the slow moving ice near the divides (Fig. 1a), questions centered around whether lakes were open or closed systems (e.g. Bell et al., 2002; Tikku et al., 2005), with considerable speculation about their impact on local ice dynamics (Dowdeswell and Siegert, 1999; Bell et al., 2007; Thoma et al., 2012).

Since 2005, a variety of repeat satellite observations of the ice surface have revealed patterns of surface uplift and subsidence consistent with the filling and draining of subglacial water bodies (e.g. Gray et al., 2005; Wingham et al., 2006; Fricker et al., 2007). In contrast to “RES lakes”, most “active lakes” have been found beneath fast flowing ice streams and outlet glaciers (Fig. 1a and b). Many of the active lakes that have been surveyed with RES (e.g. Christianson et al., 2012; Siegert et al., 2013; Wright et al., 2014) lacked the characteristic basal reflections (hydraulic flatness, specularity, and brightness relative to surroundings; see Carter et al., 2007) traditionally used to distinguish subglacial lakes. These discrepancies appear to result from qualitative differences between active lakes and RES lakes. It is believed that active lakes might have a greater impact on ice dynamics, by their location under the fast-flowing ice streams and their ability to episodically hold back and then release large volumes of water into the subglacial environment. So far only two episodes of temporary ice acceleration correlating with subglacial lake drainage events have been reported, on Byrd Glacier (Stearns et al., 2008) and Crane Glacier (Scambos et al., 2011).

Critical to resolving the link between ice dynamics and lake activity is determination of the mechanism by which lake drainage occurs. While some ice sheet models (Johnson and Fastook, 2002; Goeller et al., 2013; Livingstone et al., 2013) have begun to incorporate primitive elements of subglacial lake dynamics, they still do not have a realistic treatment of observed lake drainage processes. R-channels have been hypothesized as a lake-drainage mechanism in Antarctica (e.g. Wingham et al., 2006; Evatt et al., 2006; Carter et al., 2009), as they are known the drain ice-dammed lakes

## Part 1: Theory

S. P. Carter et al.

Title Page

Abstract

Introduction

Conclusions

References

Tables

Figures

◀

▶

◀

▶

Back

Close

Full Screen / Esc

Printer-friendly Version

Interactive Discussion



in temperate glacial environments. More recently however several complimentary lines of evidence have called into question the ability of an R-channel to form (Hooke and Fastook, 2007) and close (Fowler, 2009) in subglacial conditions typical of Antarctica, the latter suggesting that channels incised into the till may be the preferred mechanism.

In this work we test an existing R-channel model (Kingslake and Ng, 2013) on a domain based upon several well-studied lakes in the Whillans/Mercer system and develop a new model for the filling and drainage of Antarctic subglacial lakes where lake drainage occurs through channels in the underlying sediment (a till-channel, or “T-channel”) and compare the lake volumes output by both models. We aim to: (i) provide better context for ongoing observations of lake volume change with respect to the subglacial hydrology, (ii) understand how lake filling and draining affects ice flow, (iii) gain insight into the discrepancies between the locations of active and RES lakes; and (iv) move towards a consistent parameterization of subglacial lake activity in ice sheet modeling.

## 2 Basal water models and subglacial lake drainage

### 2.1 Antarctic basal water models

Models for subglacial water transport and distribution include at least one of three categories: distributed sheet flow; groundwater; and channelized flow. The simplest and most common models for ice sheet basal water flow (e.g. Le Brocq et al., 2009) tend to invoke some form of distributed system that spreads water laterally. In such systems, water pressure increases with water flux and while basal traction decreases. More sophisticated models, however, prefer to accommodate sliding by deformation of the subglacial till, making basal traction decrease through increasing till porosity (e.g. Tulaczyk, 2000). Given that subglacial till is widely understood to lack the transmissivity necessary to accommodate the water fluxes at the base of the Antarctic ice sheet (Alley, 1989), changes in till water storage have been accommodated by exchange

Title Page

Abstract

Introduction

Conclusions

References

Tables

Figures



Back

Close

Full Screen / Esc

Printer-friendly Version

Interactive Discussion



with a distributed system (e.g. Christoffersen et al., 2014; Bougamont et al., 2014). These more sophisticated distributed/groundwater exchange modes show the most consistency with borehole (Engelhardt and Kamb, 1997; Christner et al., 2014) and seismic observations (Blankenship et al., 1987) of the basal environment.

Channelized systems are those in which water flux is concentrated in one or more low-pressure conduits. These conduits, often referred to as “R-channels,” are thermally-eroded into the ice by turbulent heat generated by water moving down a hydraulic gradient (Rothlisberger, 1972; Nye, 1976). As the relative area of the ice bed interface occupied by these systems is small, they can support lower water pressures. The relative efficiency of these systems for evacuating water can also draw water away from surrounding distributed systems leading to a net slowdown of the ice as these systems evolve. This slowdown is especially pronounced in areas where the supply of water varies temporally and where surface slopes are steep enough that channels erode quickly when melt water supply is high and then lose pressure when supply subsequently dwindles (e.g. Sundal et al., 2011). The drop of water pressure in the channelized system then pulls water away from adjacent distributed systems (Andrews et al., 2014). Due to the requirement of turbulent heat for initiating “R-channels” and time varying input for the more significant pressure variations, this process has received far more consideration for the steeply-sloped margins of Greenland where the subglacial system receives a substantial portion of the meltwater from surface ablation (e.g., Pimentel and Flowers, 2011; Schoof, 2010; Werder et al., 2013). In contrast, the basal water system for most of Antarctica does not receive surface meltwater and is often at low hydraulic slopes, such that the heat generated by water moving down gradient is likely not sufficient to erode an R-channel (Alley, 1989), and channelization has therefore typically not been considered in basal water models for Antarctica (e.g. Bougamont et al., 2011; Le Brocq et al., 2009). In the last few years, however, increased consideration has been given to the possibility of channels incised in the sediments instead of the overlying ice (e.g. Van der Wel et al., 2013; Kryke-Smith and Fowler, 2014), and

## Part 1: Theory

S. P. Carter et al.

[Title Page](#)[Abstract](#)[Introduction](#)[Conclusions](#)[References](#)[Tables](#)[Figures](#)[◀](#)[▶](#)[◀](#)[▶](#)[Back](#)[Close](#)[Full Screen / Esc](#)[Printer-friendly Version](#)[Interactive Discussion](#)

to the role of channelization in the drainage of subglacial lakes (e.g. Evatt et al., 2006; Carter et al., 2009).

## 2.2 Lake-drainage theory

Most of our understanding of the drainage of subglacial lakes comes from studies of glacial-dammed lakes on temperate glaciers in alpine environments (e.g. Clarke, 2003; Werder et al., 2013) where floods descend 100s of meters over 1 to 10s of km on timescales of days and channelization is well documented (Roberts, 2005). Fowler (1999) explained the repeated drainage in these systems with the following model (see also Fig. 2): (a) when the lake is at low stand, water is trapped behind a local maximum in hydraulic potential, known as “the seal”, (b) as lake water levels rise, a hydraulic connection forms over “the seal” initiating thermal erosion by outflow from the lake, (c) during the early stages of lake drainage, the potential gradient is relatively steep and effective pressure is low causing melt to exceed creep closure, (d) with ongoing drainage, the level of the lake lowers causing a decrease in the hydraulic gradient, while the effective pressure at the seal increases, allowing the channel to continue to siphon outflow despite the lake level being lower. The effective pressure change also increases the rate of creep closure of the channel by the overlying ice, while the energy available for thermal erosion simultaneously decreases, (e) as the channel closure rate increases, a reduction in effective pressure ultimately re-forms a seal between the lake and points downstream.

Antarctic subglacial floods occur on larger spatial and longer temporal scales than alpine subglacial floods: water typically descends 10s of meters over 100s of km and drainage sometimes persists for multiple years (Wingham et al., 2006; Fricker et al., 2007). Lakes beneath Antarctica are isolated from the atmosphere and limited evidence from boreholes indicates that water travels via distributed systems (e.g. Engelhardt and Kamb, 1997; Carter et al., 2009). Although the patterns of lake volume, and outflow over time is qualitatively similar to those observed during the drainage of alpine-ice dammed lakes, recent work has shown that R-channels are unlikely to play



## Part 1: Theory

S. P. Carter et al.

Title Page

Abstract

Introduction

Conclusions

References

Tables

Figures



Back

Close

Full Screen / Esc

Printer-friendly Version

Interactive Discussion



a major role in the Antarctic subglacial water system for several reasons: (a) a substantial number of the flow paths that drain known subglacial lakes flow up an adverse bedslope from thicker ice into thinner ice where the pressure melting point is higher. Alley et al. (1998) showed that once the basal slope exceeds 1.2–1.7 times the surface slope, the heat generated by turbulent dissipation will be insufficient to maintain the water at the pressure melting point let alone melt surrounding ice, (b) most models for R-channel formation imply that the surrounding ice is temperate and isothermal. In polar ice where the temperature decreases with distance from the bed, turbulent heat generated will go first into heating the ice before melting ice, (c) creep closure of R-channels requires a drop in water pressure on the order of several 10's of meters, 5–10 times higher than the surface drawdown observed during the drainage of most Antarctic subglacial lakes (Fowler, 2009). By replacing a channel incised into the overlying ice with one incised into the sediment we address issues (a) and (b) as the erosion of sediment is less temperature sensitive than the erosion of ice and (c) because the deformability of sediment is sensitive to smaller changes in water pressure than deformability of ice (Fowler, 2009).

In this paper we develop, test, and compare models for lake drainage via an R-channel (Kingslake and Ng, 2013) alongside a model with in which channels are formed via mechanical erosion of underlying till (“T-channels”) on a domain with geometry similar to that found for flowpaths draining Antarctic subglacial lakes. We tested the output from these models with observations to see which one was able to reproduce estimates of the inferred timing and magnitude for subglacial lake drainage events most closely.

### 3 Model description

We developed two models for this work, each based on the same parameters but with a different module for channelization. Our first model (henceforth the “R-channel model”) is adapted directly from a formulation presented by Kingslake and Ng (2013)

## Part 1: Theory

S. P. Carter et al.

Title Page

Abstract

Introduction

Conclusions

References

Tables

Figures

◀

▶

◀

▶

Back

Close

Full Screen / Esc

Printer-friendly Version

Interactive Discussion



for a lake drained by a combined distributed system and R-channel as the patterns of ice flow predicted in that work appear qualitatively similar to observed ice flow associated with lake drainages in Antarctica (e.g. Stearns et al., 2008). Our second model replaces R-channels with channels mechanically incised into the underlying deformable till (henceforth “T-channel”). We derive formulations for erosion, deposition, and creep closure from theoretical work presented in Walder and Fowler (1994) and Ng (1998, 2000).

By comparing the lake volume time series output by the combined R-channel model and the T-channel model, we can (i) perform a diagnostic test for Fowler (2009)’s statement that drainage could occur for sediments that behave like erodible-deformable ice, (ii) develop tools to predict future lake drainage, and a potential prototype for incorporating lake drainage in ice sheet basal hydrology models; and (iii) form a conceptual basis for coupling more complex models of sediment and water dynamics.

### 3.1 Theory for subglacial water flow

#### 3.1.1 Subglacial water flow

Subglacial water flows from areas of high hydraulic potential to areas of lower hydraulic potential. Hydraulic potential,  $\theta$ , at the base of the ice is the sum of the water’s elevation  $z_b$  and water pressure, which at the base of ice is equal to the overburden pressure, minus the effective pressure  $N$  (Shreve, 1972):

$$\theta = z_b + (z_s - z_b) \frac{\rho_i}{\rho_w} - \frac{N}{\rho_w g} \quad (1)$$

Given that  $z_s$  and  $z_b$  can be easily measured remotely, while measuring  $N$  requires either borehole or seismic measurement, we introduce the term  $\theta_0$  which refers to the hydraulic potential when  $N = 0$ . Although many ice-sheet scale water models (e.g. Le Brocq et al., 2009; Carter et al., 2011) use only  $\theta_0$  for determining the direction of water flow, Fowler (1999) and subsequent works (Evatt et al., 2006; Fowler, 2009)

Title Page

Abstract

Introduction

Conclusions

References

Tables

Figures

◀

▶

◀

▶

Back

Close

Full Screen / Esc

Printer-friendly Version

Interactive Discussion



have shown that  $N$  is critical for process scale models of subglacial lake drainage by first of all allowing for the formation of a temporary hydraulic divide between the lake and points downstream while the lake is filling that is not present when the lake is draining. Inclusion of this term also allows water to overcome local minima in  $\theta$  along the flowpath of up to about 3 m.w.e.

Given that  $\theta$ , and  $N$ , as well as channel aperture ( $S$ ), and water flux ( $Q$ ) are each defined differently for the R-channel, T-channel and sheet flow systems, we will use the subscripts  $R$ ,  $T$ , and  $S$ , respectively to avoid confusion in the following sections. Explanations for all symbols not defined explicitly in the text can be found in Tables 1 and 2.

## 3.2 Subglacial channel formation

### 3.2.1 Channels incised into the ice (R-channels)

In the classic R-channel model transmissivity is controlled by aperture, which is controlled by a balance of erosion  $m_R$  and viscous deformation  $C_V$  such that

$$\frac{\partial S}{\partial t} = \frac{m}{\rho} - C_V \quad (2)$$

where

$$m_R = Q_R \frac{\rho_w g (1 - k_h) \frac{\partial \theta_R}{\partial x} + k_h \rho_w g \frac{\partial z_b}{\partial x} + k_h \frac{\partial N_R}{\partial x}}{L_h} \quad (3)$$

describes the conversion of turbulent heat dissipation into melting and

$$C_{VR} = K_R S_R N_R^n \quad (4)$$

describes creep closure ( $C_{VR}$ ) as a function of effective pressure and aperture size. Conservation of mass governs the change in flux along the flow by

$$\frac{\partial Q_R}{\partial x} = m_R \left( \frac{1}{\rho_w} - \frac{1}{\rho_i} \right) + C_{VR} + T_R, \quad (5)$$

where the source term  $T_R$  (Kingslake and Ng, 2013) is defined with the equation

$$T_R = R_K k (N_R - N_S). \quad (6)$$

Pressure down the channel co-evolves with water flux through an adaptation of the Manning friction formula

$$\frac{\partial N_R}{\partial x} = \rho_w g \left( f_r \frac{Q_R |Q_R|}{S_R^{\frac{8}{3}}} - \frac{\partial \theta_R}{\partial x} \right). \quad (7)$$

### 3.2.2 Conduits incised in the till

Our model for channelization by mechanical erosion into the sediments is composed of many elements of models for R-channels thermally incised into the ice (e.g. Fowler, 1999; Evatt et al., 2006; Kingslake and Ng, 2013), but borrows formulas for net erosion and viscous closure from Walder and Fowler (1994) and Ng (2000). Although more complex and presumably more precise mathematical language for conduits incised at least partially into the sediment has been introduced by Hewitt et al. (2011), van der Wel et al. (2013) and Kryke-Smith and Fowler (2014), this simplified model can act as a basis for these higher order process models. As with the R-channel, transmissivity for a till channel is governed by aperture ( $S_T$ ). Change in aperture is a balance of net erosion ( $E_T - D_T$ ) and viscous sediment deformation ( $C_{VT}$ ), such that

$$\frac{\partial S_T}{\partial t} = (E_T - D_T) - C_{VT}, \quad (8)$$

with erosion ( $E_T$ ) defined by

$$E_T = K_{T1} \frac{v_s}{\alpha_T} \left( \frac{\max(\tau_T - \tau_C, 0)}{g d_{15} (\rho_T - \rho_W)} \right)^{\frac{3}{2}}, \quad (8a)$$

and deposition ( $D_T$ ) defined by

$$D_T = K_{T2} \frac{v_s}{\alpha_T} \bar{c} \sqrt{g d_{15} \tau_T (\rho_T - \rho_W)}. \quad (8b)$$

Within these equations the characteristic sediment settling velocity ( $v_s$ ) defined by:

$$v_s = d_{15}^2 \frac{2(\rho_T - \rho_W)g}{9\mu_w} \quad (8c)$$

5 and the shear stress exerted by the water on the sediments ( $\tau_T$ ) is

$$\tau_T = |1/8 f_T \rho_W \mu_T| \quad (8d)$$

while the critical shear stress  $\tau_C$  is

$$\tau_C = 0.05 \cdot d_{50} g (T - w). \quad (8e)$$

10 Closure occurs via viscous till creep  $C_{VT}$ , though this may in reality be a convenient continuum representation of discrete till collapse events on the sides of the channel:

$$C_{VT} = \text{sgn}(N_T) \frac{A_T S_T (|N_T|/a)^a}{2N_\infty^b}, \quad (9)$$

15 where a higher value of  $A_T$  relative to  $K_R$  (see Sect. 3.4.3) allows for more rapid channel closure at higher water pressures (Walder and Fowler, 1994; Fowler, 2009). The term  $\alpha_T$  (Eqs. 8a, 8b) is a correction factor (between 5500 and 233 000) that was introduced to account for the geometric differences between the semicircular channel geometry implied by the formulation and the actual geometry which is likely more elliptical in nature (e.g. Ng, 2000; Winberry et al., 2009; Van der Wel et al., 2013). The term  $N_\infty$  (Eq. 9) refers to till effective pressure and is treated as a constant for this work (Ng, 2000); this is a simplifying assumption that we explore in more detail in Sect. 4.2.1.

[Title Page](#)[Abstract](#)[Introduction](#)[Conclusions](#)[References](#)[Tables](#)[Figures](#)[⏪](#)[⏩](#)[◀](#)[▶](#)[Back](#)[Close](#)[Full Screen / Esc](#)[Printer-friendly Version](#)[Interactive Discussion](#)

By this system of equations, channel growth via erosion is a function of water velocity and is sensitive to the sediment size and the channel geometry. Moreover, a channel can only be eroded once water exceeds a threshold velocity. At lower water fluxes channels in the will not form and sheet flow will dominate. Channel closure via deformation is a function of the effective pressure of the water ( $N_T$ ) and sensitive to the till strength ( $N_\infty$ ).

Conservation of mass is accomplished with:

$$\frac{\partial Q_T}{\partial x} = \frac{m_T}{1/\rho_w - 1/\rho_T} + C_{VT} + T_T; \quad (10)$$

$T_T$  is determined by the effective pressure difference between the till channel and the distributed sheet via

$$T_T = R_{KT} k(N_T - N_S). \quad (10a)$$

Finally we define the propagation of effective pressure along flow using conservation of momentum:

$$\frac{\partial N_T}{\partial x} = \rho_w g \left( f_T \frac{Q_T |Q_T|}{S_T^{8/3}} - \frac{\partial \theta_T}{\partial x} \right), \quad (11)$$

where we initially have  $f_{-T}$ , assuming a semicircular channel geometry.

### 3.2.3 Distributed sheet flow

The distributed or sheet flow system, common to both the combined R-channel and T-channel model is governed by three primary equations: two concern the conservation of mass; a third governs the evolution of  $N$  (Sect. 3.1.1). Water flux,  $Q_s$  is function of

the hydraulic gradient ( $\partial\theta_S/\partial x$ ) and cross sectional area ( $S_S$ ),

$$Q_S = S_S \left( \frac{\pi R_1}{4K_{S1}} \right)^{2/3} \sqrt{\frac{6.6\rho_w g}{f_r}} \partial\theta_S/\partial x, \quad (12)$$

assuming flowpath width,  $y_S$ , at any point constant with depth, such that water flux increases linearly with water layer thickness  $h_S$ . Evolution of  $S_S$  is governed by the conservation of mass by:

$$\frac{\partial S_S}{\partial t} = M_C - \frac{\partial Q_S}{\partial x} - T_{SR}, \quad (13)$$

meaning water layer thickness and transmissivity (Eq. 12) increase linearly with water storage. If water pressure is equal to overburden pressure then the only way for a water layer to clear obstacles is to thicken until it overtops them. Most subglacial water in Antarctica is, however, at pressures on the order of several meters water equivalent (10–100 s of kPa) below overburden pressure, the difference defined by the effective pressure  $N_S$ , which is inversely proportional to water thickness, by

$$N_S = \left[ \frac{\pi R_1 c_S n^n}{4K_0} \left( \frac{\tau_b^p}{S_S} \right) \right]^{\frac{1}{n+q}} \quad (14)$$

### 3.3 Simplifying assumptions

For a lake, we assume that the hydraulic potential is the sum of the bed elevation and overburden pressure (from the height of the ice column) at the centre of the lake and that it changes uniformly. With the subscript  $L$  referring to conditions as the flowpath crosses the source lake, the change in lake level with time is defined as

$$dz_b/dt_L = dz_{srf}/dt_L. \quad (15)$$

Title Page

Abstract

Introduction

Conclusions

References

Tables

Figures

◀

▶

◀

▶

Back

Close

Full Screen / Esc

Printer-friendly Version

Interactive Discussion



Change in lake volume is calculated as

$$\frac{\partial \theta_L}{\partial t} = H_L \frac{Q_{in} - Q_{out}}{A_L}, \quad (16)$$

where  $A_L$  is lake area (which is held constant in both models, i.e. we assume for simplicity that there is no change in area as the lake state changes and explore the implications of that assumption in Sect. 4.2.3),  $Q_{in}$  is inflow,  $Q_{out}$  is outflow, and  $H_L$ , a number between 1 and 2 depending on the degree to which the overlying ice is supported by bridging stresses, effectively a simplification of the parameterization of surface deformation in Evatt et al. (2007). Rather than addressing the precise number of channels we assume that there is only one channel present. Based on earlier runs of both models and assertions in Shoemaker (2002) we assume that the destination lake is the nearest major low in the hydraulic potential (empirically determined to be deeper than 3 m.w.e.). We neglect changes in the destination lake's level and assume that  $N = 0$  at its center. For the running of the till channel model we also assume: (i) viscous till behavior (Till channel only), (ii) no change in till water content or rheology over time, (iii) neglected bridging stresses, (iv) neglected downstream sediment transport and other modes of till deformation.

These systems of Eqs. (2)–(16) are solved on a 1-dimensional finite difference domain, consisting of a source lake, intermediate points, and a destination lake. The point at which  $\theta_0$  reaches a maximum is termed “the seal” and is treated as immobile in contrast to its definition in some higher-order models (e.g. Fowler, 1999; Clarke, 2003) which define the seal as the location where transmissivity is lowest at any given time.

### 3.4 Model implementation

#### 3.4.1 Model spin up and initialization

Given our initial uncertainties about the onset of channelization it is simpler to run our model when the source lake is filling, such that outflow is minimized, and the lake level



5

10

15

20

25

is well below high stand. We initialize the model assuming that water pressure equals overburden pressure and that there is a constant supply of meltwater MC along the flowpath downstream of the lake. With these initial values, we calculate the initial water layer thickness, assuming  $N_S = 0$ , reworking Eq. (2) such that,

$$S_S = \frac{Q_S}{\left(\frac{\pi R_1}{4K_{S1}}\right)^{2/3} \sqrt{\frac{6.6\rho_w g}{\tau_r}} \partial\theta_S / \partial x}. \quad (12a)$$

We then use Eq. (4) to calculate a new value for  $N_S$ , based on  $S_S$  and Eq. (3). For each subsequent time step we calculate  $Q_S$  (Eq. 2),  $\partial S_S / \partial t$  (Eq. 3), as well as change in lake properties (Eqs. 15, 16). With the resulting new water layer thickness, we finally recalculate  $N_S$  and  $S_S$ .

### 3.4.2 Criteria for onset and cessation of channelization

Initially water will flow from the seal, towards the lake; as the lake level and lake hydraulic potential increase, however, water will begin flow out of the lake over the seal. Due to the inverse relationship between  $N_S$  and  $Q_S$ , the outflow will initially be much lower than  $Q_{in}$ . We assume that the initial outflow does not erode a channel at the seal but remains as sheet flow. Only once  $Q_S$  exceeds a critical value do we allow for channelization to occur, a criterion implicitly suggesting that  $\tau_T$  must exceed a critical threshold ( $\tau_c$ ) before mechanical erosion is possible. Walder (1982) suggested that erosion will tend to concentrate in a spatially-limited area at which point increasing erosion leads to increasing channel depth; our formulation implies this as well. Once channelization is initiated, we assume the instantaneous presence of a proto-channel between the lake exit and the next lake downstream with  $Q_R = Q_S = Q_{onset}$  ( $Q_T = Q_S = Q_{onset}$ ) and  $N_R = N_S$  ( $N_T = N_S$ ). These initial values then allow us to calculate an initial  $S_R$  ( $S_T$ ) through algebraically reworking Eq. (10) (Eq. 11).

Cessation of channelization occurs once  $Q_R$  ( $Q_T$ ) falls below a threshold value,  $Q_{cessation}$ , at which point it becomes computationally simpler to eliminate the channel-

Title Page

Abstract

Introduction

Conclusions

References

Tables

Figures

◀

▶

◀

▶

Back

Close

Full Screen / Esc

Printer-friendly Version

Interactive Discussion



ization and revert back to sheet flow. Although it is possible that small incipient channels are always present such as is parameterized by Flowers et al. (2004), ignoring them improves computational speed. In Sect. 4.2, we explore in more detail how variations in  $Q_{\text{onset}}$  and  $Q_{\text{cessation}}$  affect model performance.

### 3.4.3 Evolution of channelized flow

Once the channel is initiated we calculate the geometry of a proto-channel (Eqs. 7, 11), assuming  $Q_R = Q_{\text{onset}}$  ( $Q_T = Q_{\text{onset}}$ ) everywhere between the source and destination lakes. After each successive iteration of Eqs. (2)–(4) (Eqs. 8–10), we recalculate  $Q_R$  and  $N_R$  ( $Q_T$  and  $N_T$ ) along the flowpath using a shooting method: beginning with an initial guess of  $Q_R$  ( $Q_T$ ) at the outflow, we use Eqs. (7) and (11) to calculate  $dN_R/dx$  ( $dN_T/dx$ ) locally on the staggered grid and the corresponding values for  $N_R$  and  $T_R$  ( $N_T$  and  $T_T$ ) at the next point downstream on the regular grid. Using these newly calculated values for  $N_R$  and  $T_R$  ( $N_T$  and  $T_T$ ), we calculate  $(dQ_R/dx)$   $(dQ_T/dx)$  on the regular grid and then  $Q_R$  ( $Q_T$ ) at the next point downstream on the staggered grid. This process is repeated downstream until we calculate  $N_R$  ( $N_T$ ) at the destination lake at which point it is a known quantity. We compare our calculated  $N_R$  ( $N_T$ ) with the “known”  $N_R$  ( $N_T$ ) to obtain a misfit. We then use a Newton’s method iteration on  $N_R$  ( $N_T$ ) at the downstream lake (treated as a function of  $Q_R$  ( $Q_T$ )) until we find a value for this that results in a satisfactorily close value for  $N_R$  ( $N_T$ ) at the destination lake. Once this value is obtained we then iterate Eqs. (2), (6), and (7) (Eqs. 8, 11, and 15) and the corresponding sheet flow evolution (Eqs. 12–14). To improve model stability we apply a modification of the Courant–Friedreich–Lewy (CFL) (Courant et al., 1928) criteria for the length of each time step such that neither  $S_S$  nor  $S_R$  ( $S_T$ ) can change by more than 5% at any time step. Resulting time steps ranged between 2 and  $10^5$  s.



### 3.5 Model executio

We tested both the combined R-channel and T-channel models, on an idealized domain in which the section between the source lake and the seal, and the seal and the destination lake are approximated with straight-line segments (Fig. 3a). This domain was based on a simplified version of the flowpath connecting the well-studied (e.g. Christianson et al., 2012) Subglacial Lake Whillans (SLW) to the Ross Sea from (Carter and Fricker, 2012; see Fig. 1b for location, 3b for comparison).  $y_s$  and  $h_i$  were held constant.  $A_L$  was set at 100 km<sup>2</sup>.  $Q_b$  was between 0.24 and 0.35 m<sup>3</sup> s<sup>-1</sup> with other values shown on Table 2. Hereafter we refer to the initial test of the T-Channel model on this idealized domain with conditions listed in Table 2 as the “control model,” the test of the R-channel on this domain as the “R-channel” test. On this idealized domain, we also ran a series of sensitivity studies for the T-channel model, exploring variations in both model parameters as well as input data, comparing the output timing, magnitude and the level at which high stand occurs relative to initial hydraulic potential of the seal vs. that output by the control model.

To demonstrate the ability of the T-channel model to reproduce the timing and magnitude of actual observed lake drainage events, we also applied it to several “real” domains for flowpaths draining lakes in lower Whillans and Mercer ice streams, including SLW (Fig. 3b), Lake Conway (SLC) and Lake Mercer (SLM) (Fig. 3c) and Lake Engelhardt (SLE) (Fig. 3d). For these domains values for elevation  $h_i$ ,  $z_b$ , and  $y_s$  are interpolated from radar-derived measurements of ice thickness and surface elevation made between 1971 and 1999 over multiple campaigns (see Carter et al., 2013; Lythe et al., 2001 for a full description). We validated the model for the period 2003 to 2009 by comparing the output lake volume time series to estimates based on ICESat-derived ice surface elevation change supplemented by MODIS image differencing for lake area determination (Fig. 1b for location; Fricker and Scambos, 2009; Carter et al., 2013).

[Title Page](#)[Abstract](#)[Introduction](#)[Conclusions](#)[References](#)[Tables](#)[Figures](#)[Back](#)[Close](#)[Full Screen / Esc](#)[Printer-friendly Version](#)[Interactive Discussion](#)

## 4 Results

### 4.1 Major themes common to all model run

#### 4.1.1 R-channels

Our R-channel model was unable to reproduce the observed timing and magnitude of floods in the domain. Although there was some thermal erosion of an opening it took nearly 10 years to grow the conduit large enough so that outflow was greater than inflow (Fig. 4). It is therefore possible that under the right conditions an R-channel might be able to grow under an ice sheet (especially if there is enough temperate ice frozen on to the base). However, once initiated, the rate at which ice deformation closed the channel shut was far too low to stop flow. These results along with the theoretical difficulties associated with R-channels described in Sect. 2.2 further confirm the need for an alternative mechanism of channelization.

#### 4.1.2 Results common to all or most T-channel model runs

The timing ( $\sim 4$  year recurrence interval) and magnitude ( $\sim 0.1\text{--}0.2\text{ km}^3$  volume change) of lake drainage predicted by the model was in the range of what was observed for lakes in the Whillans/Mercer ice streams (e.g. Fricker et al., 2007; Smith et al., 2009). Outflow via the distributed system was closely correlated with lake volume, peaking slightly before the lake reached high stand. Most of the outflow, however, was by the channelized system, which could maintain a monotonically decreasing hydraulic potential pathway through the seal as water level in the lake declined and the gradient in the distributed system directed water from the seal back toward the source lake.

In all model runs lake drainage began when  $\theta_0$  was still well below  $\theta_0$  at the seal (Fig. 4a), consistent with findings in (Christianson et al., 2012) and (Siegert et al., 2014) that active lakes high stands would not be at the floatation heights of their dams.

### Part 1: Theory

S. P. Carter et al.

Title Page

Abstract

Introduction

Conclusions

References

Tables

Figures

◀

▶

◀

▶

Back

Close

Full Screen / Esc

Printer-friendly Version

Interactive Discussion



## Part 1: Theory

S. P. Carter et al.

Title Page

Abstract

Introduction

Conclusions

References

Tables

Figures



Back

Close

Full Screen / Esc

Printer-friendly Version

Interactive Discussion



Although the onset of outflow before lake levels reach the floatation height has long been observed and modeled for ice marginal lakes in alpine glaciers (e.g. Fowler, 1999) and the Grimsvöt caldera lake beneath the Vatnajökull ice cap in Iceland (Björnsson, 2003; Evatt et al., 2007), this is the first time this relation between high stand and seal level has been shown in Antarctica and has been found to hold true for several real lakes.

In many of the model runs the amplitude of the filling and draining cycle decreased over time in contrast to experiments in Fowler (1999) and Evatt et al. (2006) in which the oscillations in volume increased. In our model this dampening of the filling/drainage cycle appears to result from the fact that outflow through the channelized system continued long after the lake reached low stand, such that the net filling rate was lower, as was the subsequent high stand. We explored this dampening in more detail in our sensitivity studies (Sect. 4.2).

### 4.1.3 Idealized vs. realistic domain

A comparison between the model output from an idealized domain and one that uses more realistic flow path geometry shows almost no qualitative difference, with recurrence interval, fluxes and volume ranges within less than 5 % of one another. The most significant difference was that the model ran six times faster on the idealized domain and appeared to be more stable. We suspect the slower performance of the model over the realistic domain is due to undulations in  $\theta_0$  between the seal and the destination lake the introduce localized pressure variations in response to changes in flow of water from upstream that require shorter adaptive time steps.

## 4.2 Model sensitivit

Outputs such as timing, magnitude, and high stand relative to floatation height were all shown to be quite variable in response changes in both flow path geometry and

input parameters. We divide our sensitivities into classes of tests relating to sediment properties, flow path geometry, model inputs, and low sensitivity parameters.

#### 4.2.1 Sensitivity to sediment and channel properties

The parameters to which the model shows the greatest sensitivity all relate to the properties of the sediments: channel geometry, grain size and till pressure ( $\alpha_T$ ,  $D_{15}$ ,  $N_\infty$ ) (Fig. 5a). Small changes to any one of these parameters can greatly affect the lake level at high stand, the magnitude of volume change, and the relative timing of drainage events. Although grain size and till pressure have been measured in individual locations (Tulaczyk et al., 1998; Engelhardt, 2004), our ability to sense channel geometry is improving (e.g. Schroeder et al., 2013), and till pressure has been inferred from seismic surveys (e.g. Blankenship et al., 1987), robust widespread measurements of these parameters at a level of precision that would be useful for this model are unlikely to be available. Moreover the variations in  $N_\infty$ , to which our model is sensitive (Fig. 5b) fall well below the errors of current measurements (boreholes, seismic). Although we could find values that result in a decent fit between the model and results (Table 2) there is an element of non-uniqueness to all these parameters especially  $\alpha_T$  and  $D_{15}$ , which are related through Eqs. (6a) and (6b). The sensitivity of our model output to small variations in these parameters also calls into question our assumption (Sect. 3.3) that they remain constant with time. While we can expect sediment size to remain constant over the time frame of the model,  $N_\infty$  is likely to be changing significantly over the duration of our model run as water is exchanged between the till pores and ice-bed interface (Christoffersen et al., 2014). When we consider our assumption that  $N_\infty$  remains constant over time in light of these results we can speculate on how variations in  $N_\infty$  over time might affect the filling and drainage cycle. Based on research on the exchange of water between the interfacial flow system and till (e.g. Christoffersen et al., 2014) we'd expect  $N_\infty$  to co-vary  $N_S$  and  $N_T$ . In this situation till strength would increase as lake level declined and  $N_T$  and  $N_S$  increased and water was removed from the surrounding till. As a result the channel might remain open longer than predicted by our model and

Title Page

Abstract

Introduction

Conclusions

References

Tables

Figures



Back

Close

Full Screen / Esc

Printer-friendly Version

Interactive Discussion



low stands would tend to last longer. A more detailed exploration of this process including in situ monitoring of till pressures may be key to improving the performance of our model.

#### 4.2.2 Sensitivity to flowpath geometry

We experimented with flow path geometry by multiplying bed elevation and hydraulic potential, while keeping the  $x$  coordinates the same, (Fig. 6a–c) and then stretching the coordinates along flow while preserving all other inputs (Fig. 6d–f). We explored both changes in total slope (Fig. 6a and d) as well as the slope between the source lake and the seal (Fig. 6b and e), and the seal and the destination lake (Fig. 6c and f). Overall it was found that steeper slopes favoured more rapid and dramatic lake drainage with the slope downstream of the seal being the most important factor. Changes to the flow path geometry upstream of the seal tended to be more important for determining the precise level at which the high stand would occur (Fig. 6b and e), with gentler slopes leading to higher high stand levels and with only a minor effect on the total volume range. This suggests that in the absence of sufficiently detailed data on the flow path geometry, the total hydraulic slope between source and destination lakes will exert a first order control on the magnitude of lake drainage; this was demonstrated for lakes drained by R-channels in Evatt et al. (2006). The height of the seal relative to the source lake will be more important for predicting the lake height at high stand.

#### 4.2.3 Inflow and lake area

At lower  $Q_{in}$ , there was an inverse linear relationship between recurrence cycle and input (Fig. 7a and b). At higher  $Q_{in}$ , greater levels of inflow initially resulted in higher lake levels at high stand as the outflow channel took longer to grow large enough to drain the higher volume of water coming in. While the higher high-stands and outflow levels initially provided a steeper hydraulic potential gradient resulting in a larger net volume loss, the higher inflow meant that the lake began experiencing a net increase

### Part 1: Theory

S. P. Carter et al.

Title Page

Abstract

Introduction

Conclusions

References

Tables

Figures



Back

Close

Full Screen / Esc

Printer-friendly Version

Interactive Discussion



## Part 1: Theory

S. P. Carter et al.

Title Page

Abstract

Introduction

Conclusions

References

Tables

Figures

◀

▶

◀

▶

Back

Close

Full Screen / Esc

Printer-friendly Version

Interactive Discussion



in volume when there was still a substantial quantity of water was leaving the lake, resulting in a lower net filling rate during the next cycle and lower high stand volume, but a larger channel at low stand. As a consequence the filling and drainage cycle became dampened more rapidly with each successive cycle for higher values of  $Q_{in}$ .

This suggests a mechanism by which channels might be able to flow through small apparent basins in the hydraulic potential, as the channel would quickly come into equilibrium if the ratio of flux to basin volume is relatively high. When we explored the effect of variations in  $A_L$ , we found similar results with smaller lakes experiencing greater ranges in elevation initially, but the range decreased as outflow and inflow came into equilibrium, once again suggesting that in lakes where  $Q_{in}/A_L$  is high, the system will likely come into equilibrium quite quickly.

Although we assume that  $A_L$  remains constant over the filling-draining cycle, it is more likely that  $A_L$  decreases with lake volume. This effect alone would only moderately affect the rate of drawdown leading to a slight increase in surface lowering relative to what would be expected in a constant  $A_L$  case. Lower lake levels, however, would lead to faster rates of channel closure, and this would partially counteract this effect. If  $N_{\infty}$  is also increasing as the lake drains and shrinks, then we may expect the system to eventually come into equilibrium at low stand until flow from upstream increased.

#### 4.2.4 Lower sensitivity parameters

Any factor which affected the relationship between sheet thickness and  $N$  whether it be surface slope,  $R_1$  or flowpath had an important influence on volume range. This is because such factors control how easily water overcomes an apparent obstacle in the hydraulic potential. Any parameter setting that made it easy for water to clear apparent barriers paradoxically had the effect reducing the total amplitude of the filling and draining cycle, favoring steady drainage by sheet flow (Fig. 8a). Conversely parameter values that made it difficult for water to overcome obstacles tended to increase the volume range and favor channelized drainage.

## Part 1: Theory

S. P. Carter et al.

Title Page

Abstract

Introduction

Conclusions

References

Tables

Figures

◀

▶

◀

▶

Back

Close

Full Screen / Esc

Printer-friendly Version

Interactive Discussion



The amount of sheet flow necessary to initiate channelization  $Q_{\text{onset}}$  had only minor effects when compared to the sheet roughness with respect to determining lake level at onset and volume range. Likewise,  $M_c$  or flow from other sources (primarily basal melt and flow from outside the flowpath) seemed to matter only when it was over an order of magnitude higher than values that would be reasonable for a location like the Whillans/Mercer ice streams. Under higher values of  $M_c$ , high stands were substantially lower but volume range was nearly unchanged (Fig. 8c). When values for  $M_c$  exceed  $0.1 \text{ m}^3 \text{ s}^{-1} \text{ km}^{-1}$  it started to affect the rate at which the source lake filled.

There were two model parameters that seemed to affect primarily how fast the model ran:  $Q_{\text{shutdown}}$  and the grid cell spacing,  $dx$  (Fig. 8b). Higher values for each of these parameters made the code run faster, in particular increasing  $dx$  increased decreased the runtime exponentially (Fig. 8d) however at values of more than 2.5 km for  $dx$  we began to see aliasing of the hydraulic potential that decreased the accuracy of the model output. Likewise for  $Q_{\text{shutdown}}$  values greater than 0.25 we began to observe premature shutdown of the channelized system.

### 4.3 Constant $Q_{\text{in}}$ on realistic domains

Although previous work by Carter et al. (2013) has shown that the filling rates for subglacial lakes vary considerably over time, we were able to roughly reproduce the elevation change time series using a constant value for  $Q_{\text{in}}$  (Table 2; Fig. 9a–d). This demonstrates the model's effectiveness for a wide number of environments (Fig. 3). In order to achieve a decent fit between the modelled and observed lake volume time series, however we had to vary the input parameters substantially from lake to lake (Table 2). We achieved a relatively reasonable agreement between modelled and observed timing and magnitude of lake volume change for SLW, SLC and SLE. Missing, however, were periods of quiescence, such as the slowdown in filling for SLE (Fig. 9b) for 2006–2008. The worst fit between model and observations occurred for SLM, for which our modeled frequency of filling and drainage events was over 50 % higher than observed. Initial work by Carter et al. (2013) suggests that the filling rate for SLM varied between

2.25 and over  $50 \text{ m}^3 \text{ s}^{-1}$  in response to variable outflow from SLC. Given the sensitivity of high stand levels and drainage processes to inflow rates in (see Sect. 4.2.3) it is likely that it is impossible to fully simulate this lake without allowing for time varying inflow.

Given the sensitivity of timing and drainage magnitude to parameters relating to the sediment properties, running the model at constant inflow may be a reasonable approximation for tuning those parameters. The assumption of constant inflow may even serve as a workable approximation in the absence of reliable data on lake activity upstream. Close reproduction of filling and drainage cycles will require precise and time varying inflow, which is outside the scope of this paper.

## 5 Discussion

The T-channel model reproduces observations in the Whillans/Mercer ice stream better than the R-channel model, and performs sufficiently well for us to believe that it is realistic. The modification of channels being incised into the sediment rather than the ice has two major implications: (i) many active lakes are shallow and only exist in the presence of saturated sediment, which could explain why these lakes are not detectable using radar sounding; and (ii) the process of lake drainage for such lakes is sensitive to the composition and strength of the underlying till, which suggests that it is sensitive to properties of the till, which indicates that models could be improved with a realistic treatment of sediment – interfacial water exchange. It also casts some doubt on the interpretation of the origin of channels observed under ice shelves (Le Brocq et al., 2013), which assumes that channels are carved into the basal ice. We expand on some of these implications in the following discussion.

Title Page

Abstract

Introduction

Conclusions

References

Tables

Figures

◀

▶

◀

▶

Back

Close

Full Screen / Esc

Printer-friendly Version

Interactive Discussion



## 5.1 The discrepancy between active and radar detected lake

There have been several recent inventories of Antarctic subglacial lakes as well as several other works (e.g. Smith et al., 2009; Siegert et al., 2013; Wright and Siegert, 2012; Wright et al., 2014), and all have noted a significant discrepancy between the locations of “RES lakes” and “active lakes”. While we attribute some of this discrepancy to the limitations of the distinct methods used for lake detection, our modeling work offers a plausible explanation: for areas where the regional surface slope (and resultant hydraulic gradient) is low, the only mechanism by which a self-enlarging conduit capable of siphoning substantial amounts of water several meters below the seal floatation height to points downstream can exist is if the channel it is incised into the sediment. The observed volume change reported for active lakes (Fricker et al., 2007, 2014; Fricker and Scambos, 2009; Smith et al., 2009) requires ice to be underlain by widespread, deformable saturated sediments. The presence of saturated sediments would inhibit positive identification of these lakes using the criteria of the Carter et al. (2007) radar classification strategy, such as specularity and brightness relative to surroundings. The angle of repose for these sediments would imply low basal slopes and shallow lakes. In shallow lakes, radar reflections off the lake bottom would impair the specularity criteria (Gorman and Siegert, 1999). A lake surrounded by saturated sediments might not be significantly brighter than its surroundings as the reflection coefficient between ice and for saturated sediments is very close to that that of ice and lake water (Schroeder et al., 2013).

## 5.2 Inclusion of lake drainage in ice sheet models

A number of recent models for ice flow have begun to predict the formation of subglacial lakes in local hydraulic potential minima (e.g. Sergienko and Hulbe, 2011; Goeller et al., 2013; Livingstone et al., 2013; Fried et al., 2014). These models all assume that these lakes simply fill until the water level reaches the floatation height of the “static seal” at which point they drain steadily through a distributed network at the ice bed interface.

Title Page

Abstract

Introduction

Conclusions

References

Tables

Figures



Back

Close

Full Screen / Esc

Printer-friendly Version

Interactive Discussion



## Part 1: Theory

S. P. Carter et al.

Title Page

Abstract

Introduction

Conclusions

References

Tables

Figures

◀

▶

◀

▶

Back

Close

Full Screen / Esc

Printer-friendly Version

Interactive Discussion



Although we cannot comment on lakes surrounded by bedrock, our models results suggest that subglacial lakes surrounded by saturated sediments will undergo cyclical pattern of filling and draining. This finding along with recent observations of ice velocity change in response to subglacial lake drainage (Stearns et al., 2008; Scambos et al., 2011; Fricker et al., 2014; Siegfried et al., 2015), indicate that this process needs to be explored more deeply, especially for ice sheet models of areas where lakes and sediments are known to exist such as the Siple Coast.

Ice sheet models would be limited in their ability to precisely reproduce observed lake drainage patterns due to issues relating to the spatial resolution of the ice surface and bedrock topography as well as the sensitivity of the lake drainage process to small changes in sediment composition and strength. With the sensitivities however comes the interesting possibility that subglacial lakes might form and be “active” in subglacial sediments under only limited circumstances. In particular the exchange of water between the till and the basal interface has been shown to affect till strength on timescales of less than a decade (e.g. Christoffersen et al., 2014; Bougamont et al., 2014). If a model can fill enclosed basins in the hydraulic potential and predict till strength evolution over timescales longer than the current observational record (10 years for the WIS lakes, Siegfried et al., 2014) it may provide some clues as to why active lakes appear only in certain locations.

Spatial variations in basal traction in areas of fast flow have previously been proposed as a mechanism for forming lakes (Sergienko and Hulbe, 2011), with lakes forming in the lee of local traction highs. More recently inversions of basal traction have inferred bands of stiff till impounding water in areas of moderate to fast flow, but usually outside the regions where active lakes are found (Sergienko et al., 2014). It may be these two different mechanisms of water storage, one stable and the other unstable, owe their existence to subtle changes in till properties. This along with findings of multiple other mechanisms of water storage beneath the Antarctic ice sheet (Ashmore and Bingham, 2014) indicate that simply modeling the filling an enclosed depression in

the hydraulic potential, while an important first step, is not sufficient to simulate the full nature and impact of lake dynamics in an ice sheet model.

Where active lakes are present, their tendency to drain primarily via a channelized system rather than a distributed one suggests that the formation and drainage of subglacial lakes in regions of fast flow actually results in net slowdown relative to lake free regions rather than acceleration over the longer term. Regions of the ice sheet underlain by active subglacial lakes, will however exhibit more variability in flow rate with peak ice velocity coinciding with peak distributed flow and peak lake volume. In chains of lakes, however the lubrication will be spatially variable over time as shown in Siegfried et al. (2015). The exact degree to which lake drainage accelerates ice flow is, however, highly dependent on longitudinal stresses, which is outside the scope of this paper.

### 5.3 Expression of channels seaward of grounding line

Recent work by Le Brocq et al. (2013) has suggested that a number of channel-like features in the surface and base of ice shelves may have originated when water thermally eroded grounded ice, showing how many of these linear features appear to correlate with locations where ice sheet subglacial water models predict outflow into the ice shelf cavity. While this correlation has interesting implications for the offshore evolution of subglacial outflow and its interaction with the ice shelf, our study casts doubt on the origin of such channels as hypothesized in the Le Brocq et al. (2013) paper. We have shown that even in temperate ice as is implicit in our model, that the low amounts of turbulent heat generated by water flowing down relatively gentle hydraulic gradients is insufficient to erode the ice fast enough to explain the observed lake volume change in a location like the Whillans/Mercer ice streams. If we assume polar ice (Hooke and Fastook, 2007) or factor in the adverse bed slopes (Fig. 3b and c) and associated supercooling that water exiting many of these lakes might encounter (e.g. Alley et al., 1998; Creyts et al., 2010; Carter et al., 2009) then the feasibility of channel incision into the overlying ice upstream of the grounding line is even less likely. If any thermal

Title Page

Abstract

Introduction

Conclusions

References

Tables

Figures



Back

Close

Full Screen / Esc

Printer-friendly Version

Interactive Discussion



erosion is taking place it would be the result of tidal inflow (e.g. Horgan et al., 2013), not subglacial outflow. Although the evolution of ice and subglacial water seaward of the grounding line is beyond the scope of this work, we do provide constraints on the mechanisms by which such features on the ice shelf surface might form.

## 6 Summary

We have developed a new model for subglacial lake drainage in the Antarctic ice streams in which channels are mechanically eroded into deformable subglacial sediment, and compared it to a previously-accepted model for an “R-channel” incised into the base of the ice through melting. Using the “T-channel” model we have been able to reproduce the timing and magnitude of subglacial lake drainage events in one of the better-studied regions of Antarctica, the Whillans/Mercer ice stream system. Due to effective pressure differences between the lake center and the “seal” lake drainage begins well before lake levels reaches floatation height, and accelerates once flow is sufficient to initiate erosion into the sediment. Peak distributed flow correlated with lake level, while channelization is dominant when the rate of volume loss is highest.

The time series output by the model is highly sensitive to small changes in the properties of the subglacial sediments, in particular those related to till water content. Given recent work on the exchange of water between sediment pores and the interfacial flow system taking place over time frames of years to decades, it is likely that there are substantial changes in till strength over the filling/drainage cycle of a subglacial lake.

The requirement of sediments for active lakes appears to explain why such lakes often fail classic radar detection criteria as lakes in such environments are often neither deep and therefore not specular (Gorman and Siegert, 1999), nor are such lakes brighter than their surroundings (Carter et al., 2007). Our results also cast some doubt on the interpretation of the origin of channels observed under ice shelves (Le Brocq et al., 2013), which relies on incision into the basal ice.

Title Page

Abstract

Introduction

Conclusions

References

Tables

Figures



Back

Close

Full Screen / Esc

Printer-friendly Version

Interactive Discussion



*Acknowledgements.* Funding for this research was provided by the Antarctic Integrated Systems Science (AISS) program of the National Science Foundation, through the WISSARD project and by the Cryospheric Sciences program at NASA.

Work also benefitted from conversations with: Geir Moholdt, David Heezel, Fernando Paolo, Adrian Borsa, Andrew Fowler, Mauro Werder, Stephen Livingstone, Ted Scambos, Dustin Schroeder, Duncan Young, Slawek Tulaczyk, Richard Alley, Jonathan Kingslake, Tim Creyts, Christian Schoof, and Ian Hewitt, and the WISSARD Team members.

## References

- Alley, R. B.: Water-pressure coupling of sliding and bed deformation. 1. Water-system, *J. Glaciol.*, 35, 108–118, 1989.
- Alley, R. B.: Towards a hydrological model for computerized ice-sheet simulations, *Hydrol. Process.*, 10, 649–660, 1996.
- Alley, R. B., Lawson, D. E., Evenson, E. B., Strasser, J. C., and Larson, G. J.: Glaciohydraulic supercooling: a freeze-on mechanism to create stratified, debris-rich basal ice: II. Theory, *J. Glaciol.*, 44, 563–569, 1998.
- Anandakrishnan, S. and Alley, R. B.: Stagnation of ice stream C, West Antarctica by water piracy, *Geophys. Res. Lett.*, 24, 265–268, 1997.
- Andrews, L. C., Catania, G. A., Hoffman, M. J., Gulley, J. D., Luthi, M. P., Ryser, C., Hawley, R. L., and Neumann, T. A.: Direct observations of evolving subglacial drainage beneath the Greenland Ice Sheet, *Nature*, 514, 80–83, doi:10.1038/nature13796, 2014.
- Ashmore, D. W. and Bingham, R. G.: Antarctic subglacial hydrology: current knowledge and future challenges, *Antarct. Sci.*, 26, 758–773, 2014.
- Bell, R. E., Studinger, M., Tikku, A. A., Clarke, G. K. C., Gutner, M. M., and Meertens, C.: Origin and fate of Lake Vostok water frozen to the base of the East Antarctic ice sheet, *Nature*, 416, 307–310, 2002.
- Bell, R. E., Studinger, M., Shuman, C. A., Fahnestock, M. A., and Joughin, I.: Large subglacial lakes in East Antarctica at the onset of fast-flowing ice streams, *Nature*, 445, 904–907, doi:10.1038/nature05554, 2007.
- Björnsson, H.: Subglacial lakes and jokulhlaups in Iceland, *Global Planet. Change*, 35, 255–271, 2003.

Title Page

Abstract

Introduction

Conclusions

References

Tables

Figures

◀

▶

◀

▶

Back

Close

Full Screen / Esc

Printer-friendly Version

Interactive Discussion



## Part 1: Theory

S. P. Carter et al.

[Title Page](#)[Abstract](#)[Introduction](#)[Conclusions](#)[References](#)[Tables](#)[Figures](#)[Back](#)[Close](#)[Full Screen / Esc](#)[Printer-friendly Version](#)[Interactive Discussion](#)

- Blankenship, D. D., Bentley, C. R., Rooney, S. T., and Alley, R. B.: till Beneath Ice Stream-B. 1. Properties derived from seismic travel-times, *J. Geophys. Res. B*, 92, 8903–8911, 1987.
- Bougamont, M. and Tulaczyk, S.: Glacial erosion beneath ice streams and ice-stream tributaries: constraints on temporal and spatial distribution of erosion from numerical simulations of a West Antarctic ice stream, *Boreas*, 32, 178–190, doi:10.1111/j.1502-3885.2003.tb01436.x, 2003.
- Bougamont, M., Price, S., Christoffersen, P., and Payne, A. J.: Dynamic patterns of ice stream flow in a 3-D higher-order ice sheet model with plastic bed and simplified hydrology, *J. Geophys. Res.*, 116, F04018, doi:10.1029/2011jf002025, 2011.
- Carter, S. P., Blankenship, D. D., Peters, M. E., Young, D. A., Holt, J. W., and Morse, D. L.: Radar-based subglacial lake classification in Antarctica, *Geochem. Geophys. Geosy.*, 8, Q03016, doi:10.1029/2006gc001408, 2007.
- Carter, S. P., Blankenship, D. D., Young, D. A., Peters, M. E., Holt, J. W., and Siegert, M. J.: Dynamic distributed drainage implied by the flow evolution of the 1996–1998 Adventure Trench subglacial lake discharge, *Earth Planet. Sc. Lett.*, 283, 24–37, doi:10.1016/j.epsl.2009.03.019, 2009.
- Carter, S. P., Fricker, H. A., Blankenship, D. D., Johnson, J. V., Lipscomb, W. H., Price, S. F., and Young, D. A.: Modeling 5 years of subglacial lake activity in the MacAyeal Ice Stream (Antarctica) catchment through assimilation of ICESat laser altimetry, *J. Glaciol.*, 57, 1098–1112, 2011.
- Carter, S. P., Fricker, H. A., and Siegfried, M. R.: Evidence of rapid subglacial water piracy under Whillans Ice Stream, West Antarctica, *J. Glaciol.*, 59, 1147–1162, doi:10.3189/2013JoG13J085, 2013.
- Carter, S. P., Fricker, H. A., and Siegfried, M. R.: Active lakes in Antarctica survive on a sedimentary substrate II: Application to the lower Whillans Ice Stream, *The Cryosphere Discuss.*, submitted, 2015.
- Christianson, K., Jacobel, R. W., Horgan, H. J., Anandkrishnan, S., and Alley, R. B.: Subglacial Lake Whillans – Ice-penetrating radar and GPS observations of a shallow active reservoir beneath a West Antarctic ice stream, *Earth Planet. Sci. Lett.*, 331, 237–245, doi:10.1016/j.epsl.2012.03.013, 2012.
- Christner, B. C., Priscu, J. C., Achberger, A. M., Barbante, C., Carter, S. P., Christianson, K., Michaud, A. B., Mikucki, J. A., Mitchell, A. C., Skidmore, M. L., Vick-Majors, T. J., and

## Part 1: Theory

S. P. Carter et al.

[Title Page](#)[Abstract](#)[Introduction](#)[Conclusions](#)[References](#)[Tables](#)[Figures](#)[Back](#)[Close](#)[Full Screen / Esc](#)[Printer-friendly Version](#)[Interactive Discussion](#)

the, W. S. T.: A microbial ecosystem beneath the West Antarctic ice sheet, *Nature*, 512, 310–313, doi:10.1038/nature13667, 2014.

Christoffersen, P., Bougamont, M., Carter, S. P., Fricker, H. A., and Tulaczyk, S.: Significant groundwater contribution to Antarctic ice streams hydrologic budget, *Geophys. Res. Lett.*, 41, 2003–2010, doi:10.1002/2014GL059250, 2014.

Courant, R., Friedrichs, K., and Lewy, H.: On the partial difference equations of mathematical physics, *IBM J. Res. Develop.*, 11, 215–234, 1967.

Creyts, T. T. and Clarke, G. K. C.: Hydraulics of subglacial supercooling: theory and simulations for clear water flows, *J. Geophys. Res.-Earth*, 115, F03021, doi:10.1029/2009jf001417, 2010.

Dowdeswell, J. A. and Siegert, M. J.: The dimensions and topographic setting of Antarctic subglacial lakes and implications for large-scale water storage beneath continental ice sheets, *Geol. Soc. Am. Bull.*, 111, 254–263, 1999.

Engelhardt, H.: Thermal regime and dynamics of the West Antarctic ice sheet, *Ann. Glaciol.*, 39, 85–92, doi:10.3189/172756404781814203, 2004.

Engelhardt, H. and Kamb, B.: Basal hydraulics system of a West Antarctic ice stream: constraints from borehole observations, *J. Glaciol.*, 43, 207–230, 1997.

Evatt, G. W. and Fowler, A. C.: Cauldron subsidence and subglacial floods, *Ann. Glaciol.*, 45, 163–168, 2007.

Evatt, G. W., Fowler, A. C., Clark, C. D., and Hulton, N. R. J.: Subglacial floods beneath ice sheets, *Philos. T. Roy. Soc. A*, 364, 1769–1794, doi:10.1098/rsta.2006.1798, 2006.

Flowers, G. E., Bjornsson, H., Palsson, F., and Clarke, G. K. C.: A coupled sheet-conduit mechanism for jokulhlaup propagation, *Geophys. Res. Lett.*, 31, L05401, doi:10.1029/2003gl019088, 2004.

Fowler, A. C.: Breaking the seal at Grimsvotn, Iceland, *J. Glaciol.*, 45, 506–516, 1999.

Fowler, A. C.: Dynamics of subglacial floods, *P. Roy. Soc. A-Math. Phys.*, 465, 1809–1828, doi:10.1098/rspa.2008.0488, 2009.

Fricker, H. A. and Scambos, T.: Connected subglacial lake activity on lower Mercer and Whillans Ice Streams, West Antarctica, 2003–2008, *J. Glaciol.*, 55, 303–315, 2009.

Fried, M. J., Hulbe, C. L., and Fahnestock, M. A.: Grounding-line dynamics and margin lakes, *Ann. Glaciol.*, 55, 87–96, doi:10.3189/2014AoG66A216, 2014.

## Part 1: Theory

S. P. Carter et al.

Title Page

Abstract

Introduction

Conclusions

References

Tables

Figures



Back

Close

Full Screen / Esc

Printer-friendly Version

Interactive Discussion



Goeller, S., Thoma, M., Grosfeld, K., and Miller, H.: A balanced water layer concept for subglacial hydrology in large-scale ice sheet models, *The Cryosphere*, 7, 1095–1106, doi:10.5194/tc-7-1095-2013, 2013.

Gorman, M. R. and Siegert, M. J.: Penetration of Antarctic subglacial lakes by VHF electromagnetic pulses: information on the depth and electrical conductivity of basal water bodies, *J. Geophys. Res.-Sol. Ea.*, 104, 29311–29320, 1999.

Hewitt, I. J.: Modelling distributed and channelized subglacial drainage: the spacing of channels, *J. Glaciol.*, 57, 302–314, doi:10.3189/002214311796405951, 2011.

Hooke, R. L. and Fastook, J.: Thermal conditions at the bed of the Laurentide ice sheet in Maine during deglaciation: implications for esker formation, *J. Glaciol.*, 53, 646–658, doi:10.3189/002214307784409243, 2007.

Horgan, H. J., Alley, R. B., Christianson, K., Jacobel, R. W., Anandakrishnan, S., Muto, A., Beem, L. H., and Siegfried, M. R.: Estuaries beneath ice sheets, *Geology*, 41, 1159–1162, 2013.

Johnson, J. and Fastook, J. L.: Northern Hemisphere glaciation and its sensitivity to basal melt water, *Quaternary Int.*, 95–96, 65–74, doi:10.1016/s1040-6182(02)00028-9, 2002.

Kapitsa, A. P., Ridley, J. K., Robin, G. D., Siegert, M. J., and Zotikov, I. A.: A large deep fresh-water lake beneath the ice of central East Antarctica, *Nature*, 381, 684–686, 1996.

Kingslake, J. and Ng, F.: Modelling the coupling of flood discharge with glacier flow during jökulhlaups, *Ann. Glaciol.*, 54, 25–31, doi:10.3189/2013AoG3163A331, 2013.

Kyrke-Smith, T. M. and Fowler, A. C.: Subglacial swamps, *P. Roy. Soc. A-Math. Phys.*, 470, 20140340, doi:0.1098/rspa.2014.0340, 2014.

Le Brocq, A. M., Payne, A. J., Siegert, M. J., and Alley, R. B.: A subglacial water-flow model for West Antarctica, *J. Glaciol.*, 55, 879–888, doi:10.3189/002214309790152564, 2009.

Le Brocq, A. M., Ross, N., Griggs, J. A., Bingham, R. G., Corr, H. F. J., Ferraccioli, F., Jenkins, A., Jordan, T. A., Payne, A. J., Rippin, D. M., and Siegert, M. J.: Evidence from ice shelves for channelized meltwater flow beneath the Antarctic Ice Sheet, *Nat. Geosci.*, 6, 945–948, doi:10.1038/ngeo1977, 2013.

Livingstone, S. J., Clark, C. D., Woodward, J., and Kingslake, J.: Potential subglacial lake locations and meltwater drainage pathways beneath the Antarctic and Greenland ice sheets, *The Cryosphere*, 7, 1721–1740, doi:10.5194/tc-7-1721-2013, 2013.

Lythe, M. B., Vaughan, D. G., Lambrecht, A., Miller, H., Nixdorf, U., Oerter, H., Steinhage, D., Allison, I. F., Craven, M., Goodwin, I. D., Jacka, J., Morgan, V., Ruddell, A., Young, N.,

## Part 1: Theory

S. P. Carter et al.

[Title Page](#)[Abstract](#)[Introduction](#)[Conclusions](#)[References](#)[Tables](#)[Figures](#)[Back](#)[Close](#)[Full Screen / Esc](#)[Printer-friendly Version](#)[Interactive Discussion](#)

Wellman, P., Cooper, A. P. R., Corr, H. F. J., Doake, C. S. M., Hindmarsh, R. C. A., Jenkins, A., Johnson, M. R., Jones, P., King, E. C., Smith, A. M., Thomson, J. W., Thorley, M. R., Jezek, K., Li, B., Liu, H., Hideo, M., Damm, V., Nishio, F., Fujita, S., Skvarca, P., Remy, F., Tesut, L., Sievers, J., Kapitsa, A., Macheret, Y., Scambos, T., Filina, I., Masolov, V., Popov, S., Johnstone, G., Jacobel, B., Holmlund, P., Naslund, J., Anandakrishnan, S., Bamber, J. L., Bassford, R., Declair, H., Huybrechts, P., Rivera, A., Grace, N., Casassa, G., Tabacco, I., Blankenship, D., Morse, D., Conway, H., Gades, T., Nereson, N., Bentley, C. R., Lord, N., Lange, M., and Sanhaeger, H.: BEDMAP; a new ice thickness and subglacial topographic model of Antarctica, *J. Geophys. Res.*, 106, 11335–311351, 2001.

Ng, F. S. L.: Canals under sediment-based ice sheets, *Ann. Glaciol.*, 30, 146–152, doi:10.3189/172756400781820633, 2000.

Nye, J. F.: Water flow in glaciers: jokulhlaups, tunnels and veins, *J. Glaciol.*, 17, 181–207, 1976.

Pimentel, S. and Flowers, G. E.: A numerical study of hydrologically driven glacier dynamics and subglacial flooding, *P. Roy. Soc. A-Math. Phys.*, 467, 537–558, doi:10.1098/rspa.2010.0211, 2011.

Pritchard, H. D., Ligtenberg, S. R. M., Fricker, H. A., Vaughan, D. G., van den Broeke, M. R., and Padman, L.: Antarctic ice-sheet loss driven by basal melting of ice shelves, *Nature*, 484, 502–505, doi:10.1038/nature10968, 2012.

Ridley, J. K., Cudlip, W., and Laxon, S. W.: Identification of subglacial lakes using ERS-1 radar altimeter, *J. Glaciol.*, 39, 625–634, 1993.

Robinson, R. V.: Experiment in visual orientation during flights in the Antarctic, *Sov. Antarct. Exped. Bull.*, 2, 233–234, 1964.

Röthlisberger, H.: Water pressure in intra- and subglacial channels, *J. Glaciol.*, 11, 177–203, 1972.

Scambos, T. A., Berthier, E., and Shuman, C. A.: The triggering of subglacial lake drainage during rapid glacier drawdown: Crane Glacier, Antarctic Peninsula, *Ann. Glaciol.*, 52, 74–82, 2011.

Schoof, C.: Ice-sheet acceleration driven by melt supply variability, *Nature*, 468, 803–806, doi:10.1038/nature09618, 2010.

Sergienko, O. V. and Hulbe, C. L.: “Sticky spots” and subglacial lakes under ice streams of the Siple Coast, Antarctica., *Ann. Glaciol.*, 52, 18–22, doi:10.3189/172756411797252176, 2011.

Shreve, R. L.: Movement of water in glaciers, *J. Glaciol.*, 11, 205–214, 1972.

## Part 1: Theory

S. P. Carter et al.

[Title Page](#)[Abstract](#)[Introduction](#)[Conclusions](#)[References](#)[Tables](#)[Figures](#)[◀](#)[▶](#)[◀](#)[▶](#)[Back](#)[Close](#)[Full Screen / Esc](#)[Printer-friendly Version](#)[Interactive Discussion](#)

Siegert, M. J., Taylor, J., and Payne, A. J.: Spectral roughness of subglacial topography and implications for former ice-sheet dynamics in East Antarctica, *Global Planet. Change*, 45, 249–263, doi:10.1016/j.gloplacha.2004.09.008, 2005a.

Siegert, M. J., Carter, S., Tabacco, I., Popov, S., and Blankenship, D. D.: A revised inventory of Antarctic subglacial lakes, *Antarct. Sci.*, 17, 453–460, doi:10.1017/s0954102005002889, 2005b.

Siegert, M. J., Ross, N., Corr, H., Smith, B., Jordan, T., Bingham, R. G., Ferraccioli, F., Rippin, D. M., and Le Brocq, A.: Boundary conditions of an active West Antarctic subglacial lake: implications for storage of water beneath the ice sheet, *The Cryosphere*, 8, 15–24, doi:10.5194/tc-8-15-2014, 2014.

Siegfried, M. R., Fricker, H. A., Roberts, M., Scambos, T. A., and Tulaczyk, S.: A decade of West Antarctic subglacial lake interactions from combined ICESat and CryoSat-2 altimetry, *Geophys. Res. Lett.*, 41, 891–898, doi:10.1002/2013GL058616, 2014.

Stearns, L. A., Smith, B. E., and Hamilton, G. S.: Increased flow speed on a large East Antarctic outlet glacier caused by subglacial floods, *Nat. Geosci.*, 1, 827–831, doi:10.1038/ngeo356, 2008.

Thoma, M., Grosfeld, K., Mayer, C., and Pattyn, F.: Ice-flow sensitivity to boundary processes: a coupled model study in the Vostok Subglacial Lake area, Antarctica, *Ann. Glaciol.*, 53, 173–180, doi:10.3189/2012AoG60A009, 2012.

Tikku, A. A., Bell, R. E., Studinger, M., and Clarke, G. K. C.: Ice flow field over Lake Vostok, East Antarctica inferred by structure tracking, *Earth Planet. Sc. Lett.*, 227, 249–261, doi:10.1016/j.epsl.2004.09.021, 2004.

Tikku, A. A., Bell, R. E., Studinger, M., Clarke, G. K. C., Tabacco, I., and Ferraccioli, F.: Influx of meltwater subglacial Lake Concordia, East Antarctica, *J. Glaciol.*, 51, 96–104, 2005.

Tulaczyk, S., Kamb, B., Scherer, R. P., and Engelhardt, H. F.: Sedimentary processes at the base of a West Antarctic ice stream: constraints from textural and compositional properties of subglacial debris, *J. Sediment. Res.*, 68, 487–496, 1998.

Tulaczyk, S., Mikucki, J. A., Siegfried, M. R., Priscu, J. C., Barcheck, C. G., Beem, L. H., Behar, A., Burnett, J., Christner, B. C., Fisher, A. T., Fricker, H. A., Mankoff, K. D., Powell, R. D., Rack, F., Sampson, D., Scherer, R. P., Schwartz, S. Y., and Team, T. W. S.: WISSARD at Subglacial Lake Whillans, West Antarctica: scientific operations and initial observations, *Ann. Glaciol.*, 55, 51–58, doi:10.3189/2014AoG65A009, 2014.

## Part 1: Theory

S. P. Carter et al.

Title Page

Abstract

Introduction

Conclusions

References

Tables

Figures

◀

▶

◀

▶

Back

Close

Full Screen / Esc

Printer-friendly Version

Interactive Discussion



van der Wel, N., Christoffersen, P., and Bougamont, M.: The influence of subglacial hydrology on the flow of Kamb Ice Stream, West Antarctica, *J. Geophys. Res.-Earth*, 118, 97–110, doi:10.1029/2012jf002570, 2013.

Walder, J. S.: stability of sheet flow of water beneath temperate glaciers and implications for glacier surging, *J. Glaciol.*, 28, 273–293, 1982.

Walder, J. S. and Fowler, A.: Channelized subglacial drainage over a deformable bed, *J. Glaciol.*, 40, 3–15, 1994.

Werder, M. A., Hewitt, I. J., Schoof, C. G., and Flowers, G. E.: Modeling channelized and distributed subglacial drainage in two dimensions, *J. Geophys. Res.-Earth*, 118, 2140–2158, doi:10.1002/jgrf.20146, 2013.

Winberry, J. P., Anandakrishnan, S., Alley, R. B., Bindschadler, R. A., and King, M. A.: Basal mechanics of ice streams: insights from the stick-slip motion of Whillans Ice Stream, West Antarctica, *J. Geophys. Res.-Earth*, 114, F01016, doi:10.1029/2008jf001035, 2009.

Wright, A. and Siegert, M.: A fourth inventory of Antarctic subglacial lakes, *Antarct. Sci.*, 24, 659–664, doi:10.1017/s095410201200048x, 2012.

Wright, A. P., Young, D. A., Bamber, J. L., Dowdeswell, J. A., Payne, A. J., Blankenship, D. D., and Siegert, M. J.: Subglacial hydrological connectivity within the Byrd Glacier catchment, East Antarctica, *J. Glaciol.*, 60, 345–352, doi:10.3189/2014JoG13J014, 2014.

Young, D. A., Wright, A. P., Roberts, J. L., Warner, R. C., Young, N. W., Greenbaum, J. S., Schroeder, D. M., Holt, J. W., Sugden, D. E., Blankenship, D. D., van Ommen, T. D., and Siegert, M. J.: A dynamic early East Antarctic Ice Sheet suggested by ice-covered fjord landscapes, *Nature*, 474, 72–75, doi:10.1038/nature10114, 2011.



Table 1. List of all symbols used in this paper with definitions.

| Symbol    | Meaning                                    | Units                          | Value/method   |
|-----------|--|--------------------------------|--|
| $A_T$     | Flow law constant for sediment             | $M^{0.47} L^{-0.47} T^{-0.94}$ | $3 \times 10^{-5} \text{ pa}^{b-a} \text{ s}^{-1}$   |
| $A_L$     | Lake area                                  | $L^2$                          | Measured   |
| $a$       | Constant of sediment deformation           | –                              | 1.33   |
| $b$       | Constant of sediment deformation           | –                              | 1.8  |
| $C_{VT}$  | Rate of viscous till closure               | $L^2 T^{-1}$                   | Output by model                                      |
| $c$       | Sediment concentration in water column     | –                              | Output by model                                      |
| $c_s$     | Constant for roughness                     | $M^3 L^4 T^5$                  | $2 \times 10^{-20} \text{ ms}^{-1} \text{ Pa}^{-3}$  |
| $D_T$     | Deposition rate                            | $LT^{-1}$                      | Output by model                                      |
| $d_{15}$  | Characteristic grain size                  | $L$                            | Input (see Table 2)                                  |
| $d_{50}$  | Median grain size                          | $L$                            | Calculated from input                                |
| $E_T$     | Erosion rate                               | $LT^{-1}$                      | Output by model                                      |
| $f_r$     | Hydraulic roughness                        | $L^{2/3} T^{-2}$               | $0.07 \text{ m}^{2/3} \text{ s}^{-2}$                |
| $f_T$     | Dimensionless friction factor              | –                              | 0.1  |
| $g$       | Gravitational acceleration                 | $LT^{-2}$                      | $9.81 \text{ ms}^{-2}$                               |
| $H_L$     | Lake Height                                | –                              | Measured/modeled                                     |
| $h_s$     | Water layer thickness for sheetflow system | $L$                            |  |
| $h_i$     | Ice thickness                              | $L$                            | Measured   |
| $K_0$     | Glenn's flow law parameter for ice         | –                              | $10^{-24} \text{ Pa}^{-3} \text{ s}^{-1}$            |
| $K_{S1}$  | Constant                                   | –                              | 1.1  |
| $K_{T1}$  | Erosional constant                         | –                              | 0.1  |
| $K_{T2}$  | Constant of deposition                     | –                              | 6  |
| $k$       | Constant of sheet – conduit transfer       | $M^{-1} L^3 T$                 | $10^{-9} \text{ m}^2 \text{ s}^{-1} \text{ Pa}^{-1}$ |
| $k_h$     |  | –                              | 0.309  |
| $L_h$     | Latent heat of fusion                      | $L^2 T^{-2}$                   | $333.5 \text{ KJ kg}^{-1}$                           |
| $M_c$     | Flux into system from melt/inflow          | $L^2 T^{-1}$                   | Carter et al. (2013)                                 |
| $m$       | Melt rate/net erosion rate                 | $ML^{-2} T^{-1}$               | Output by model                                      |
| $N$       | Effective pressure                         | $MT^{-2} L^{-1}$               | Output by model                                      |
| $n$       | Glenn's flow law exponent                  | –                              | 3  |
| $p$       | Constant for power law sliding             | –                              | 4  |
| $Q_b$     | Base flow in distributed system            | $L^3 T^{-1}$                   | Carter et al. (2013)                                 |
| $Q_{in}$  | Inflow to lake                             | $L^3 T^{-1}$                   | Carter et al. (2013)                                 |
| $Q_{out}$ | Outflow from lake                          | $L^3 T^{-1}$                   | Output by model                                      |
| $Q_s$     | Outflow via distributed system             | $L^3 T^{-1}$                   | Output by model                                      |
| $Q_R$     | Outflow via R channels                     | $L^3 T^{-1}$                   | Output by model                                      |

## Part 1: Theory

S. P. Carter et al.

Title Page

Abstract

Introduction

Conclusions

References

Tables

Figures

◀

▶

◀

▶

Back

Close

Full Screen / Esc

Printer-friendly Version

Interactive Discussion



Table 1. Continued.

| Symbol                | Meaning  | Units            | Value/method                                      |
|-----------------------|--|------------------|---|
| $Q_T$                 | Outflow via T channels   | $L^3 T^{-1}$     | Output by model                                   |
| $Q_{\text{onset}}$    | Outflow necessary for channel initiation                               | $L^3 T^{-1}$     | Input (see Table 2)                               |
| $Q_{\text{shutdown}}$ | Outflow below which channelization ceases                              | $L^3 T^{-1}$     | Input (see Table 2)                               |
| $q$                   | Constant for power law sliding   | –                | 1   |
| $R_1$                 | Characteristic obstacle height   | L                | Input (see Table 2)                               |
| $R_k$                 | Coefficient for transmission efficiency between conduits and sheetflow | –                | Input (0.05)                                      |
| $S_s$                 | Cross sectional area of sheetflow system                               | $L^2$            | Output by model                                   |
| $S_T$                 | Till Channel cross sectional area                                      | $L^2$            | Output by model                                   |
| $T_{\text{sr}}$       | Flux between sheetflow and channelized systems                         | $L^2 T^{-1}$     | Output by model                                   |
| $t$                   | time   | T                | Measured  |
| $u$                   | Mean water velocity downstream   | $L T^{-1}$       | Output by model                                   |
| $v_s$                 | Mean setting velocity  | $L T^{-2}$       | Calculated  |
| $x$                   | Along flow distance  | L                | Measured  |
| $y_S$                 | Crossflow distance   | L                | Measured  |
| $z_b$                 | Ice base elevation   | L                | Measured initially, but changes with model output |
| $z_s$                 | Ice surface elevation  | L                | Measured initially, but changes with model output |
| $\alpha_T$            | Geometry correction  | –                | Input (see Table 2)                               |
| $\theta$              | hydraulic potential  | L                | Measured/calculated                               |
| $M_w$                 | Viscosity of water   | $ML^{-1} T^{-1}$ | $1.787 \times 10^{-3}$ pas                        |
| $\rho_w$              | Density of water   | $ML^{-3}$        | $1000 \text{ kg m}^{-3}$                          |
| $\rho_i$              | Density of ice   | $ML^{-3}$        | $917 \text{ kg m}^{-3}$                           |
| $\rho_s$              | Density of sediment  | $ML^{-3}$        | $2700 \text{ kg m}^{-3}$                          |
| $\tau_b$              | Basal driving stress   | $ML^{-1} T^{-2}$ | Calculated from initial measurements              |
| $\tau_c$              | Critical hydraulic shear stress necessary to initiate erosion          | $ML^{-1} T^{-2}$ | Calculated  |
| $\tau_T$              | hydraulic shear stress necessary to initiate erosion                   | $ML^{-1} T^{-2}$ | Output by model                                   |

## Part 1: Theory

S. P. Carter et al.

**Table 2.** List of parameters used for each of the experiments.

|                                 | Idealized/<br>Control | R-channel | SLW               | SLE               | SLC               | SLM               |
|---------------------------------|-----------------------|-----------|-------------------|-------------------|-------------------|-------------------|
| $\alpha T$                      | $6.0 \times 10^3$     | N/A       | $1.9 \times 10^4$ | $2.3 \times 10^5$ | $1.3 \times 10^4$ | $6.0 \times 10^3$ |
| $d_{15}$ (mm)                   | 0.12                  | N/A       | 0.24              | 1.5               | 0.25              | 0.12              |
| $Q_{in}$ ( $m^3 s^{-1}$ )       | 5                     | 5         | 4                 | 16                | 12                | 22.5              |
| $Q_{onset}$ ( $m^3 s^{-1}$ )    | 0.75                  | 0.75      | 1.75              | 1.25              | 3.5               | 0.75              |
| $Q_{shutdown}$ ( $m^3 s^{-1}$ ) | 0.25                  | 0.25      | 0.25              | 0.25              | 0.25              | 0.25              |
| $R_1$ (mm)                      | 6.0                   | 6.0       | 6.0               | 24                | 1.5               | 6.0               |
| $A_L$ ( $km^2$ )                | 100                   | 100       | 58                | 257               | 247               | 132               |
| $N_{\infty}/\rho_w g$ (m w.e.)  | 2.5                   | N/A       | 3.25              | 9                 | 1.75              | 2.5               |
| $H_L$                           | 2                     | 2         | 2                 | 1                 | 1                 | 2                 |
| $M_C$ ( $m^3 s^{-1}/0.001$ km)  | 0.001                 | 0.001     | 0.013             | 0.025             | 0.002             |                   |

Title Page

Abstract

Introduction

Conclusions

References

Tables

Figures

I◀

▶I

◀

▶

Back

Close

Full Screen / Esc

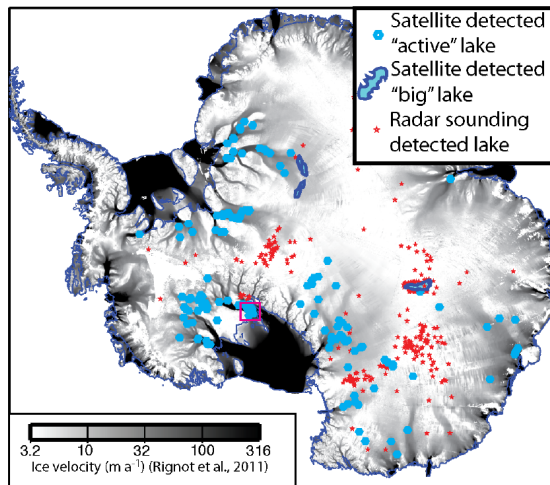
Printer-friendly Version

Interactive Discussion

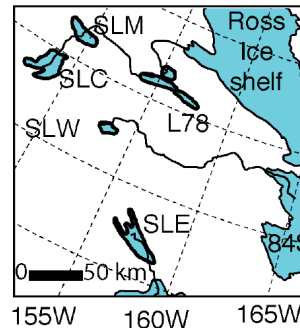


[Title Page](#)[Abstract](#)[Introduction](#)[Conclusions](#)[References](#)[Tables](#)[Figures](#)[◀](#)[▶](#)[◀](#)[▶](#)[Back](#)[Close](#)[Full Screen / Esc](#)[Printer-friendly Version](#)[Interactive Discussion](#)

a location map

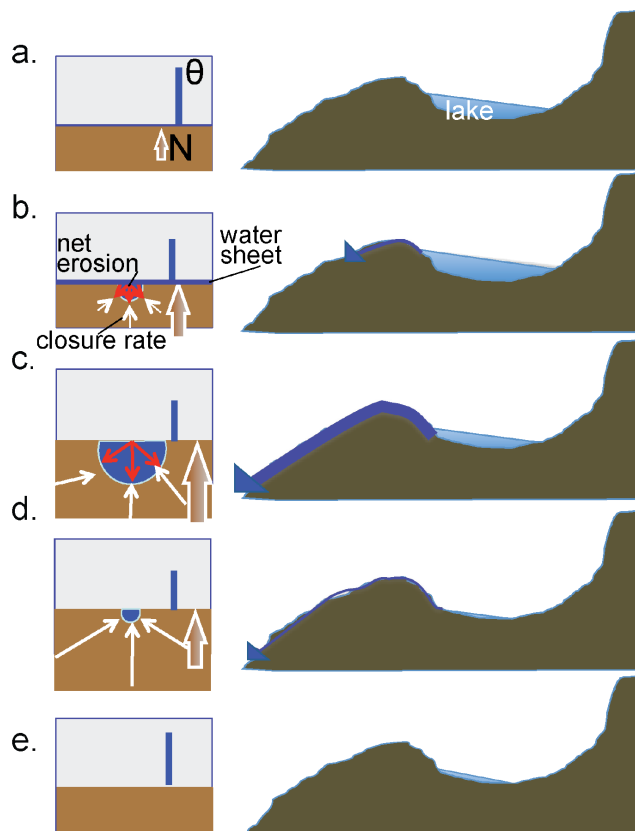


b Study area



**Figure 1.** Map of study area showing (a) location map and inventory of “RES” vs. “Active lakes” (Wright and Siegert, 2012) with a colour scale indicating ice velocities from (Rignot et al., 2011). (b) Map of lakes and flowpaths used in this study.

[Title Page](#)
[Abstract](#)
[Introduction](#)
[Conclusions](#)
[References](#)
[Tables](#)
[Figures](#)

[Back](#)
[Close](#)
[Full Screen / Esc](#)
[Printer-friendly Version](#)
[Interactive Discussion](#)


**Figure 2.** Schematic diagram showing the basic principles of our model.

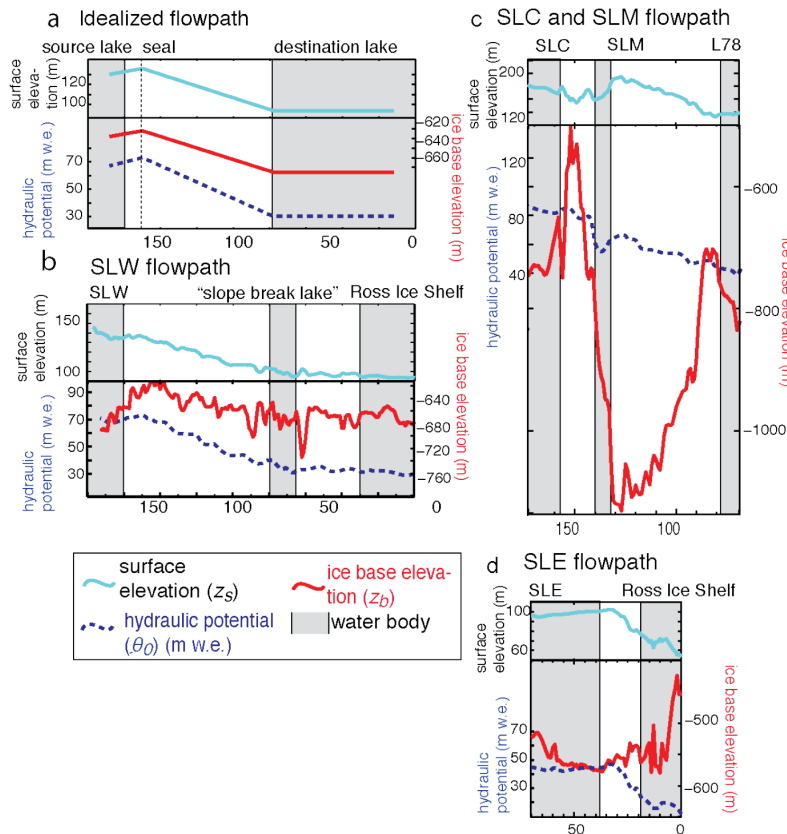


**Figure 3.** Ice surface elevation, hydraulic potential, and ice base elevation along the (a) the idealized lake flowpath, (b) the flowpath draining SLW (from Carter and Fricker, 2012), (c) the flowpath draining SLC and SLM, and (d) the flowpath draining SLE.

## Part 1: Theory

S. P. Carter et al.

Title Page

Abstract

Introduction

Conclusions

References

Tables

Figures

◀

▶

◀

▶

Back

Close

Full Screen / Esc

Printer-friendly Version

Interactive Discussion

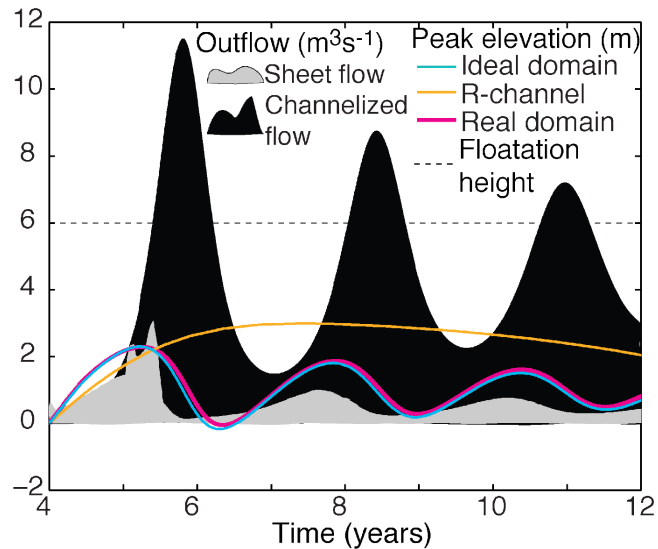


**Figure 4.** Results of steady inflow model on idealized and realistic domains (see Fig. 3a and b respectively).

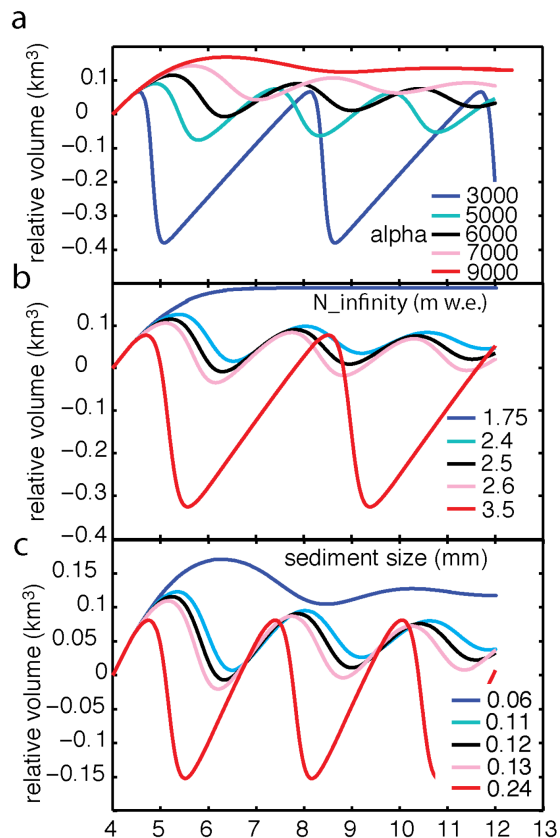


**Figure 5.** Results of a sensitivity study testing how model output varies in response to changes in (a)  $\alpha_T$ , (b)  $N_{\infty}$ , and (c)  $d_{15}$ . Black line denotes “control” run common to all sensitivity studies plotted.



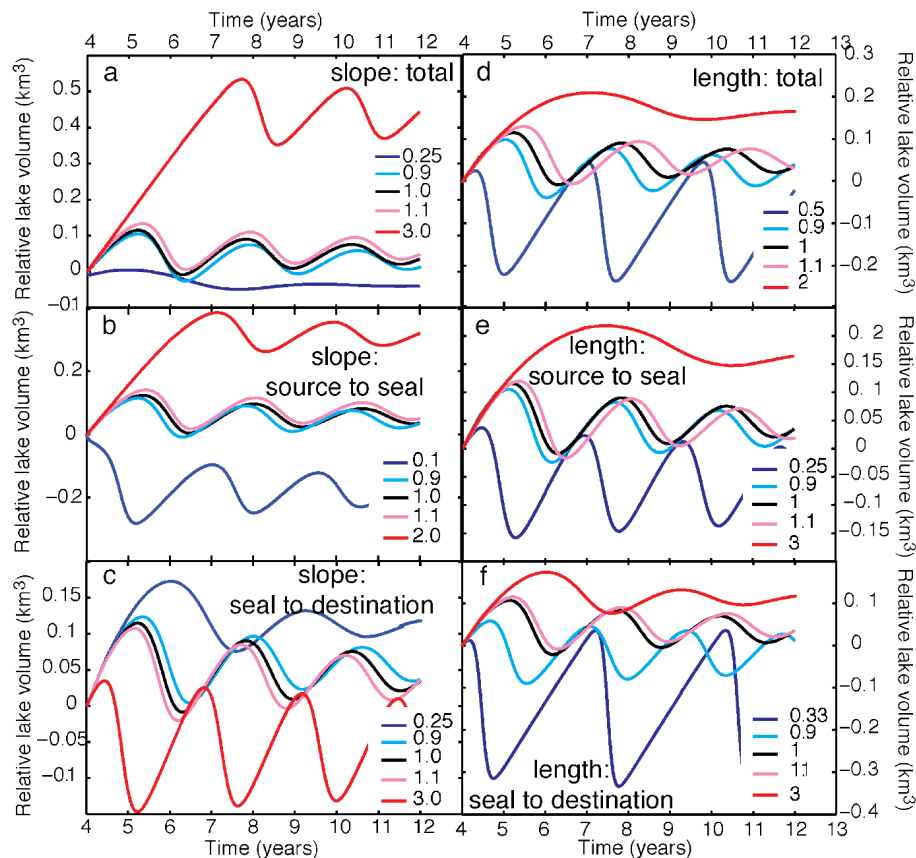


**Figure 6.** Variation of model output in response to changes in model geometry: **(a)** total vertical exaggeration, **(b)** vertical exaggeration upstream of seal, **(c)** vertical exaggeration downstream of seal, **(d)** total horizontal exaggeration, **(e)** horizontal exaggeration upstream of seal, **(f)** horizontal exaggeration downstream of seal.

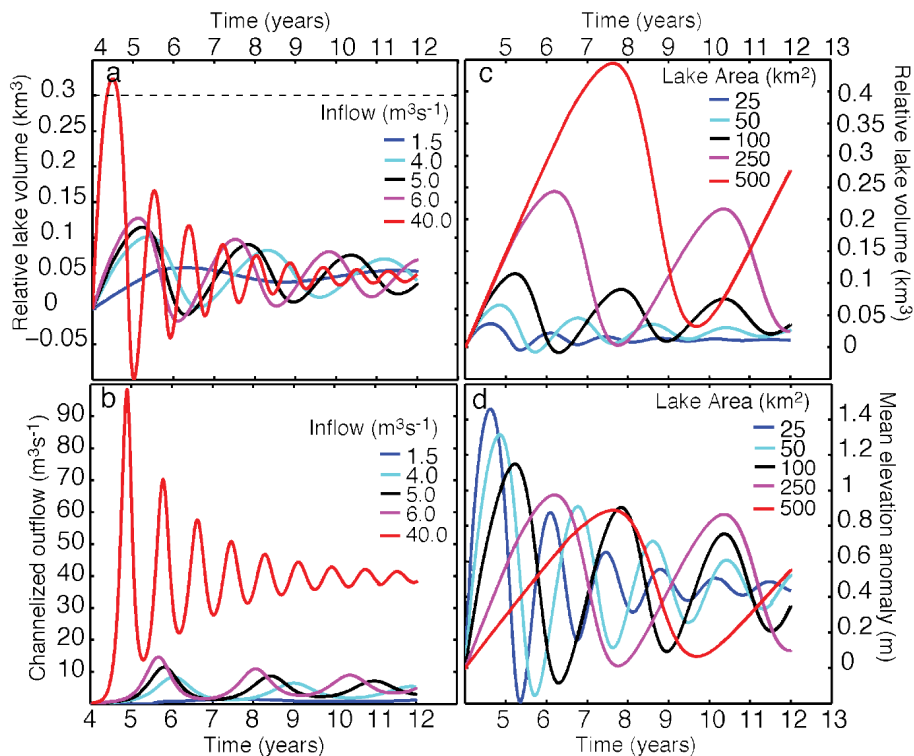


**Figure 7.** Sensitivity of **(a)** lake volume change over time and **(b)** channelized outflow ( $Q_T$ ) to variations in inflow  $Q_{in}$ . Sensitivity of **(c)** lake volume change over time and **(d)** mean lake surface elevation to variations in lake area  $A_L$ .

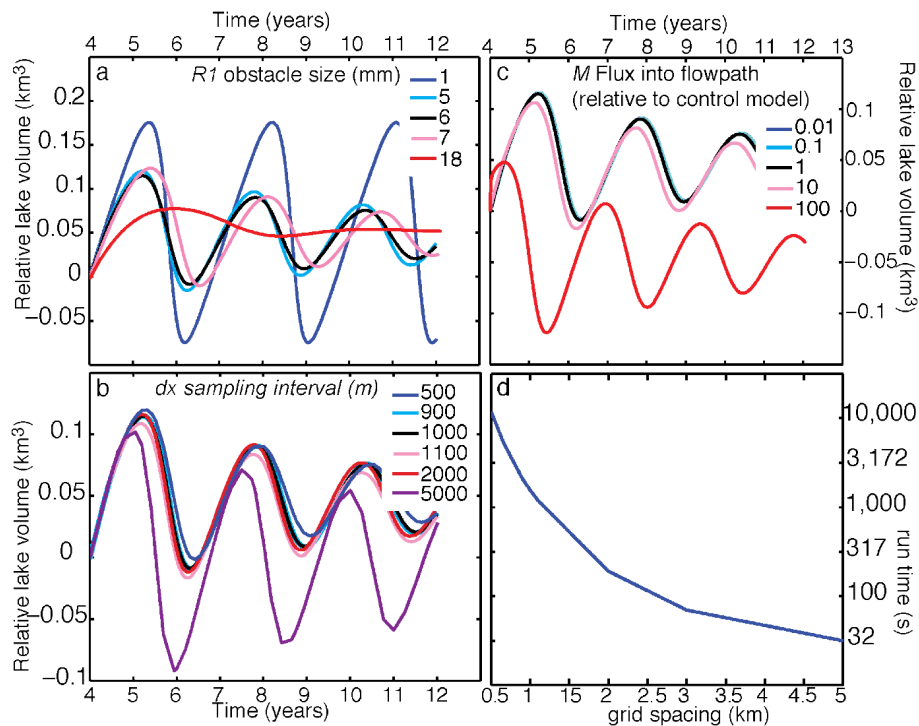


**Figure 8.** Sensitivity of modelled volume change to (a) R1 obstacle size, (b) sampling interval, and (c) water flux into the flowpath. (d) comparison of model run time for different sampling intervals.

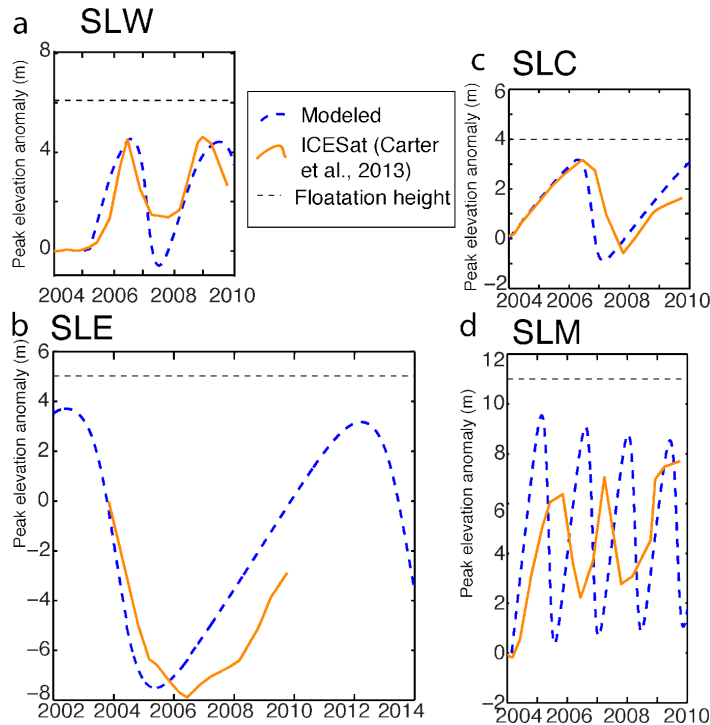


**Figure 9.** Plot of modelled and observed lake evolution showing mean lake surface elevation (observed and modelled), and outflow via distributed and channelized systems (modelled) for constant  $Q_{in}$  runs for **(a)** SLW, **(b)** SLE, **(c)** SLC, and **(d)** SLM.

Title Page

Abstract Introduction

Conclusions References

Tables Figures

◀ ▶

◀ ▶

Back Close

Full Screen / Esc

Printer-friendly Version

Interactive Discussion

